Nanoscale

RSC Publishing

PAPER

View Article Online
View Journal | View Issue

Non-enzymatic oxalic acid sensor using platinum nanoparticles modified on graphene nanosheets†

Cite this: *Nanoscale*, 2013, **5**, 5779

Xiaomei Chen,*[ac] Zhixiong Cai,[d] Zhiyong Huang,[a] Munetaka Oyama,[c] Yaqi Jiang[b] and Xi Chen*[b]

An enzyme-free oxalic acid (OA) electrochemical sensor was assembled using a platinum nanoparticle-loaded graphene nanosheets (PtNPGNs)-modified electrode. The PtNPGNs, with a high yield of PtNPs dispersed on the graphene nanosheets, were successfully achieved by a green, rapid, one-step and template-free method. The resulting PtNPGNs were characterized by transmission electron microscopy (TEM), high-resolution TEM, energy-dispersive X-ray spectroscopy, X-ray photoelectron spectroscopy, and an X-ray diffraction technique. Electrochemical oxidation of OA on the PtNPGNs-modified electrode was investigated by cyclic voltammetry and differential pulse voltammetry methods. Based on the results, the modified electrode exhibited high electrochemical activity with well-defined peaks of OA oxidation and a notably decreased overpotential compared to the bare or even the GNs-modified electrode. Under optimized conditions, a good linear response was observed for the concentration of OA and its current response was in the range of 0.1–15 mM and 15–50 mM with a detection limit ($S/N = 3$) of 10 μM. Furthermore, the electrochemical sensor presented good characteristics in terms of stability and reproducibility, promising the applicability of the sensor in practical analysis.

Received 18th February 2013
Accepted 21st March 2013

DOI: 10.1039/c3nr00848g

www.rsc.org/nanoscale

Introduction

Oxalic acid (OA) naturally occurs in many plants and can be easily combined with Ca^{2+} or Mg^{2+} to form less soluble salts. High levels of these salts in the diet lead to irritation of the digestive system, especially of the stomach and kidneys.[1] Therefore, the detection of OA in food and urine has a great significance in practice. Electrochemical OA sensors, especially enzymatic biosensors, hold a leading position among various biosensors.[2–4] The majority of these biosensors are based on the use of oxalate oxidase (OxOx), which specially catalyzes the oxidation of OA to CO_2 and H_2O_2. Although some of these enzyme-based sensors show good selectivity and high sensitivity, originating from the enzyme characteristics, the most common and serious problem with enzymatic OA sensors is insufficient long-term stability. In addition, since the sensor sensitivity essentially depends on the enzyme activity, reproducibility is still a critical issue in quality control.

Direct electrocatalytic oxidation of OA at an enzyme-free electrode would exhibit conveniences and advantages that avoid the enzyme electrode drawbacks. Recently, the interest in a practical OA electrochemical sensor has been centered on the efforts to find a breakthrough in electrocatalysts. In this context, various substrates, such as massive materials (Pd,[5] glassy carbon,[6] boron-doped diamond,[1] *etc.*), modified nanoparticles such as PdNPs/PAMAM-MWCNTs,[7] AuNPs/MWCNTs,[8] CNTs,[9] SiO_2/C/CoPc,[10] *etc.*, have been studied. On the basis of these studies, it is shown that the oxidation of OA is influenced deeply by the electrode type as well as its surface and composition. Therefore, efforts need to be made to find new materials with high electrochemical activity and large surface areas to achieve a good response to OA.

Platinum is well-known for its excellent catalytic activity towards several electrochemical processes, including the oxidation of OA.[11–13] To obtain higher surface areas and reduce the cost of the catalyst, various methods for the preparation of the Pt-catalyst have been reported, such as by immobilizing Pt nanopaticles (PtNPs) on the surface of conductive support materials.[14–17] Graphene nanosheets (GNs) exhibit a structure of 2D sheets composed of sp^2-bonded carbon atoms with one or more atomic thickness and possess a theoretical surface area of 2630 $m^2\ g^{-1}$, which surpass that of graphite (10 $m^2\ g^{-1}$), and is two-folds larger than that of carbon nanotubes (1315 $m^2\ g^{-1}$).[18,19] Therefore, GNs have received considerable interest for immobilizing nanoparticles on them.[20–22]

[a]*College of Biological Engineering, Jimei University, Xiamen, 361021, China. E-mail: xmchen@jmu.edu.cn; Fax: +86-592-6180470; Tel: +86-592-6181487*

[b]*State Key Laboratory of Marine Environmental Science, Xiamen University, Xiamen, 361005, China. E-mail: xichen@xmu.edu.cn; Fax: +86-592-2184530; Tel: +86-592-2184530*

[c]*Department of Material Chemistry, Graduate School of Engineering, Kyoto University, Nishikyo-ku, Kyoto, 615-8520, Japan*

[d]*Ministry of Education Key Laboratory of Analysis and Detection Technology for Food Safety, Fuzhou University, Fuzhou, 350002, China*

† Electronic supplementary information (ESI) available. See DOI: 10.1039/c3nr00848g

In our previous study, we found a facile method to synthesize highly active palladium nanoparticles (PdNPs)[23] and platinum nanoflowers (PtNFs)[24] on graphene oxide (GO) nanosheets, respectively. In further research, we found that the PtNPs can be easily and directly prepared on the GNs by modification of the previous method. Taking advantage of the well-dispersed, high-yield, "clean" surface (template-free preparation) and large surface area of the PtNPs, and the high conductivity of the GNs, the nano-composite revealed an unusually high electrocatalytic activity and excellent performance for OA determination. In order to verify the sensor reliability, it was applied to the determination of water-soluble OA in spinach samples. The satisfactory results confirmed the sensor applicability in practical analysis. To our knowledge, this is the first work focused on constructing PtNPGNs for non-enzymatic OA sensing.

Experimental section

Materials

K_2PtCl_4 was purchased from Wako Pure Chemicals, Co. Ltd (Japan); graphite powder, ethanol, $HClO_4$ and OA were from Lvyin Co. (China); 5% Nafion ethanol solution and PtC catalyst were from Aldrich Chem. Co. (USA) and disk glassy carbon electrodes (GCEs) were from BAS Co. Ltd (Japan). All other reagents were of analytical grade and used without further purification. The pure water for solution preparation was from a Millipore Autopure WR600A system (USA).

Instrumentation

The morphologies and crystal structures of the PtNPGNs observed by TEM and high-resolution TEM (HRTEM), which were performed on a JEM-2100 transmission electron microscopy with an acceleration voltage of 200 kV. All TEM samples were prepared by depositing a drop of diluted suspension in ethanol on a copper grid coated with a carbon film. The phases of the as-prepared products were determined by means of the powder X-ray diffraction (XRD) pattern, recorded on a Panalytical X-pert diffractometer with Cu Kα radiation. Electronic binding energies of C1s and Pt4f were measured by X-ray photoelectron spectroscopy (XPS) analysis, which was performed on a PHI Quantum 2000 Scanning ESCA Microprobe with a monochromatic microfocused Al X-ray source. All the binding energies were calibrated by C1s as the reference energy (C1s = 284.6 eV). Cyclic voltammetry (CV) and differential pulse voltammetry (DPV) measurements were performed with a CHI 660B Electrochemical Analyzer. A conventional three-electrode system included a GCE coated with the PtNPGNs film, a silver auxiliary electrode and a saturated calomel reference electrode (SCE).

Procedures

GO was prepared according to a modified Hummer's method.[25,26] For the reduction of GO, 50 mg of the as-synthesized GO was dispersed in 100 mL water to obtain a yellow-brown aqueous solution with the aid of ultrasonication. GNs were achieved by heating the GO solution in an oil bath at 100 °C for 24 h.[27]

In a typical synthesis of the PtNPGNs, a mixture of the homogeneous GNs suspension (0.1 mL 0.5 mg mL^{-1}), K_2PtCl_4 (0.15 mL 10 mM) aqueous solution and 2.5 mL ethanol was kept in a vial under vigorous stirring for 60 min. Then, the reaction mixture was washed with pure water and centrifuged to remove the remaining reagents. To compare the electrochemical activity of OA oxidation, the PtNFs were produced according to our previous report.[24]

Before the preparation of the sensor, a GCE was polished with 1, 0.3 and 0.05 μm α-Al_2O_3, sequentially. In the coating of the GC electrode surface with the PtNPGNs nano-composite, 20 μL of the PtNPGNs suspension was dispersed in a certain volume of 0.5% Nafion ethanol solution, then a certain volume of the mixture was deposited on the polished GC electrode and dried in the air for 4 h at room temperature (see more details in Scheme 1). To prepare the GNs/Nafion-GC, PtC/Nafion-GC and PtNFs/Nafion-GC electrodes, 20 μL of the nano-materials were dispersed in 20 μL 0.5% Nafion ethanol solution, respectively. After ultrasonication, 4 μL of the mixture was deposited on the polished GC electrode and dried in the air for 4 h at room temperature.

For the preparation of spinach samples, 5 g samples were cut into small pieces and extracted with 10 mL pure water in a boiling water bath for 20 min. The suspension was centrifuged at 2500 rpm for 6 min, and the supernatant filtered through filter paper. The residue retained by the filter was treated twice with 10 mL pure water and then filtered. The combined filtrates were mixed and diluted to 100 mL with 0.1 M $HClO_4$. Finally, a suitable sample solution was analyzed to find its water-soluble OA content.

Results and discussion

Characterization of the PtNPGNs composite

The preparation strategy of the PtNPGNs composite is shown in Scheme 1. The PtNPGNs composite could be obtained easily through stirring the mixture containing GNs, Pt precursor and ethanol under room temperature (30 °C) for 1 h. Fig. 1A–C shows the representative TEM images of the product at different magnifications. Low-magnification TEM image (Fig. 1A) shows that all the PtNPs were uniformly dispersed on the GN surface. The absence of isolated PtNPs in the product indicates strong interactions between the GNs and PtNPs. The magnified image (Fig. 1B) shows that the average size of these PtNPs was about 4 nm, furthermore, every two or three PtNPs tend to aggregate to

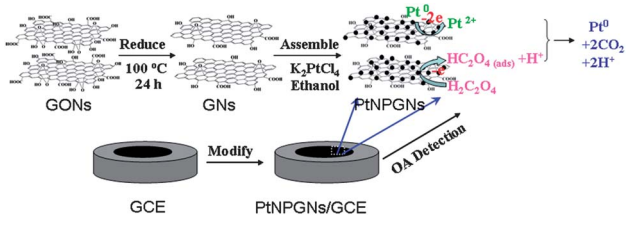

Scheme 1 Schematic illustration of the preparation of the PtNPGNs nano-composite and its application in OA determination.

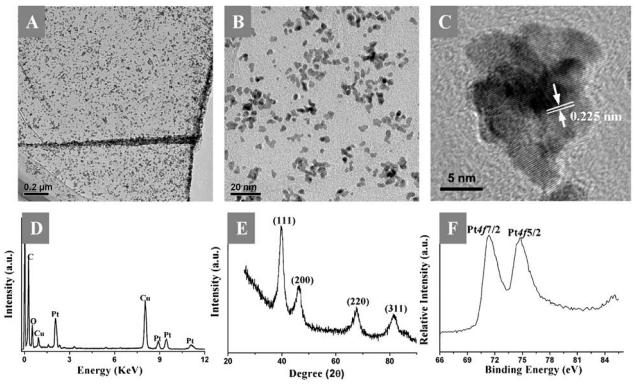

Fig. 1 (A–C) Representative TEM (A and B) and HRTEM (C) images of the PtNPGNs composite. (D–F) The EDX (D), XRD (E) and Pt4f XPS spectra (F) of the as-synthesized PtNPGNs composite.

form a nanodendrite structure. The HRTEM image (Fig. 1C) indicates that the PtNPs presented a single-crystalline structure. The interplanar spacing is 0.225 nm, which agrees well with the (111) lattice spacing of face-centered-cubic (fcc) Pt (0.225 nm). Fig. 1D shows a typical EDX analysis of the prepared PtNPGNs composite, in which an obvious Pt peak could be found, suggesting that the PtNPs were successful attached to the surface of the GNs . The formation of the PtNPGNs composite was further characterized by XRD (Fig. 1E) and XPS (Fig. 1F) techniques. In the XRD spectra, the strong diffraction peaks at $2\theta = 39.6°$, 46.2°, 67.5°, and 81.4° can be assigned to the characteristic (111), (200), (220), and (311) crystalline planes of Pt (JCPDS: 87-0647), respectively. XPS patterns of the resulting PtNPGNs composite show significant Pt4f signals corresponding to the binding energy of Pt^0, which further supported the conclusion that the PtNPs were effectively assembled on the surface of the GNs.

Electrocatalytic oxidation of OA

The CV method was used to compare and investigate the electrochemical behavior of the prepared PtNPGNs/Nafion-GCE. Fig. 2A presents the CV responses on a PtNPGNs/Nafion-modified electrode in 0.1 M $HClO_4$ solution, with and without 10 mM OA. The current–potential profile of the modified electrode in the $HClO_4$ solution was almost featureless. During the positive potential scan, the major redox process includes an anodic peak at 0.55 V, corresponding to the formation of platinum oxides and a single sharp cathodic peak at about 0.38 V, corresponding to the reformation of a clean surface of Pt^0. In comparison, the CV curve for OA in solution was complicated. A new and well-defined oxidation peak, located at 1.05 V, was shown in the curve, however, the cathodic peak at 0.38 V was obviously decreased. The former could be attributed to the electro-oxidation of OA on the PtNPGNs/Nafion-modified electrode. Previous studies have pointed out that at higher potentials, the oxidation of OA involves a direct homogeneous chemical reaction between $HC_2O_4^-$ and metal ions generated on the electrode surface.[11,28] In this regard, OA molecules tend to be oxidized on the PtNPGNs/Nafion-GCE as detailed in Scheme 2.

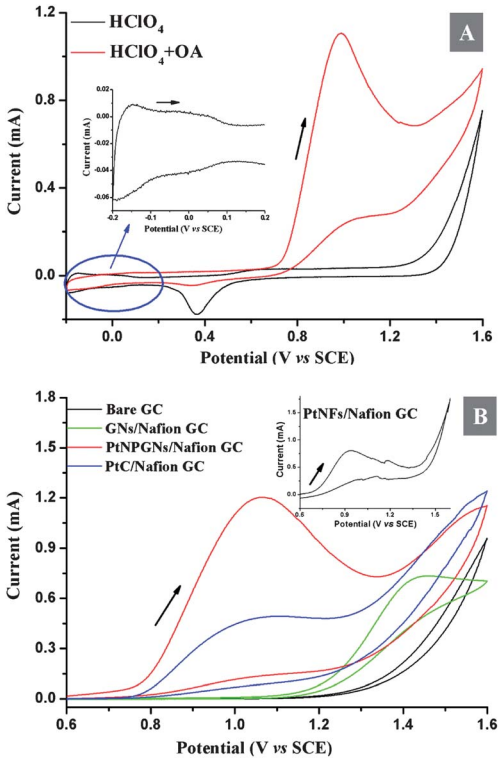

Fig. 2 (A) CV curves of the PtNPGNs/Nafion-GCE in solution, with and without OA. The inset shows the enlarged curve between −0.2 and 0.2 V in $HClO_4$ solution. (B) CV curves in $HClO_4$–OA solution on different electrodes. The inset shows the CV curve of the PtNFs/Nafion-GCE. Scan rate: 60 mV s^{-1}; $HClO_4$: 0.1 M; OA: 10 mM.

According to the process, the electrochemically generated platinum ions are rapidly reduced in the presence of OA, which inhibits the reduction of platinum oxides to Pt^0, resulting in the suppression of the cathodic peak.

We further investigated the effect of different electrode materials on OA oxidation. Fig. 2B shows a comparison of the results of the voltammograms obtained from OA oxidation by a bare GC, a GNs/Nafion-GC, a PtNPGNs/Nafion-GC, a PtC/Nafion-GC and a PtNFs/Nafion-GC (the inset) electrode. It should be pointed out that a slow but continuous decrease of electrode activity was observed during the applied potential scanning from −0.2 to 1.6 V on PtNPGNs/Nafion-GCE, whereas, the electrode response remains essentially constant after repetitive potential scanning when the applied potential was scanned between 0.6 and 1.6 V. This result revealed that adsorption of the reactant and/or intermediate oxidation products on the electrode surface at a lower potential would lead to the fouling of catalytic sites, with subsequent continuous diminution of electrode activity; on the other hand, at a

$$H_2C_2O_4 \rightarrow HC_2O_{4(ads)}^- + H^+$$
$$Pt \rightarrow Pt^{II} + 2e^-$$
$$Pt^{II} + HC_2O_{4(ads)}^- \rightarrow Pt + 2CO_2 + H^+$$

Scheme 2 Oxidation procedures of OA on the PtNPs.

higher applied potential, the absence of adsorption processes or the rapid electro-oxidation of intermediate products will maintain the integrity of the catalytic activity. Therefore, in this experiment, the initial potential of 0.6 V was selected. It has been reported that the OA reaction mechanism is highly dependent on the nature of the electrode material. When the interaction of OA molecules with the electrode surface is particularly strong, the oxidation reaction is fast.[11,29,30] As can be seen from the CV curves, the onset potential of OA oxidation on the bare GCE and the GNs/Nafion-GCE was 1.25 V and 1.10 V, respectively, which is more positive than that on the Pt modified electrode (<0.7 V). This result suggests that Pt significantly affects the electrocatalytic oxidation of OA, and the reaction rate determined on these electrodes decreases as follows: PtNFs > PtNPGNs > PtC. Although the overpotential on PtNFs/Nafion-GCE is more negative than that on PtNPGNs/Nafion-GCE, the voltammetric response is not stable due to the serious oxygen evolution. Moreover, the current density (J) of the OA oxidation peak on the PtNPGNs/Nafion-GCE is 6.50 mA cm^{-2}. The value is 1.67- and 2.30-fold greater than that obtained for the PtNFs/Nafion-GCE and PtC/Nafion-GCE, respectively (Table S1†). Generally, a higher electro-oxidation current density indicates the superior electrocatalytic activity of the electrode. These results illustrate that the PtNPGNs/Nafion-GCE presented the best catalytic performance among the five electrodes tested.

Performance of the electrochemical sensor for OA detection

To improve the performance of the non-enzymatic OA sensor, several factors such as the acidic media, PtNPGNs/Nafion amounts and the ratio of Nafion to PtNPGNs were optimized. When the PtNPGNs/Nafion-GCE was used in 0.1 M HCl, the OA reaction is rather inhibited by chloride anions. However, when the experiment was carried out in 0.5 M H_2SO_4, a fast voltammetric response to OA oxidation can be obtained, but the current peak was lower than that in $HClO_4$, which is in accordance with the Pt electrocatalytic activity being higher in perchloric than in sulfuric acid at pH < 2.5.[11,28] As a result, 0.1 M $HClO_4$ was selected as the supporting electrolyte.

The ratio of Nafion to PtNPGNs and the PtNPGNs/Nafion amount on the electrode greatly affected the sensitivity and stability of the sensor (Fig. 3). Too much Nafion decreases the electrode conductivity, and the sulfonic groups on Nafion prevent the absorption of $HC_2O_4^-$ from the PtNPGNs surface, resulting in the decrease in current response. On the other hand, if the amount of Nafion is not enough, the composite film will easily crack away from the electrode. The results, as shown in Fig. 3, display that a 1 : 1 ratio of Nafion to PtNPGNs gives the optimal composition for OA detection. We further investigated the effect of the PtNPGNs/Nafion amount on the OA sensing. More PtNPGNs/Nafion coated on the electrode meant more electroactive sites towards OA electro-oxidation, leading to a higher current peak, however, the stability of the sensor was poor when the PtNPGNs/Nafion amount was more than 4 μL.

The optimal experimental conditions, 4 μL PtNPGNs/Nafion with the ratio of Nafion to PtNPGNs at 1 : 1 were selected to provide high sensitivity and a stable DPV signal for OA sensing

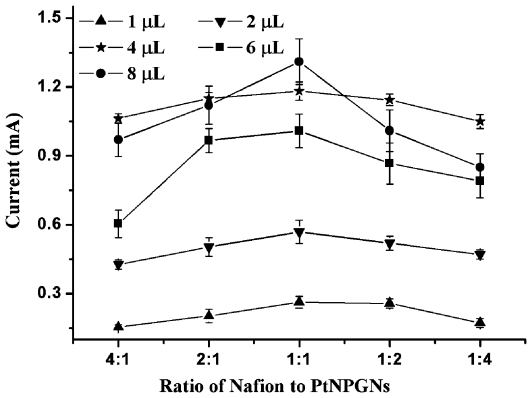

Fig. 3 Effect of PtNPGNs/Nafion amounts and the ratio of Nafion to PtNPGNs on the detection system. $HClO_4$: 0.1 M; OA: 10 mM; DPV conditions: amplitude, 50 mV; pulse width, 20 ms; pulse period, 200 ms.

in 0.1 M $HClO_4$. Fig. 4 demonstrates the DPV responses of the PtNPGNs/Nafion-GCE towards different concentrations of OA. The peak currents increased linearly with the increasing of OA concentration in two ranges of 0.1 to 15 mM and 15 to 50 mM (the inset (a) of Fig. 4) with a detection limit ($S/N = 3$) of 10 μM. It is obvious that the slope of the OA concentration in the 0.1 to 15 mM range is larger than that in 15 to 50 mM. Moreover, the potential peaks shift positively with the increasing of OA concentration. These results indicated that the detection sensitivity became lower with an increase of OA concentration. Although PtNPs with "clean" surfaces show high electrocatalytic activity in OA electro-oxidation, during the detection, PtNPs can also be gradually poisoned by the adsorption of molecules, which affect the detection sensitivity. It should be pointed out that the oxygen-containing groups of the GNs can improve the tolerance of the PtNPs to some extent, so the poisoning is not so serious for OA detection. In the preparation of the OA sensor in our laboratory, involving 10 different GCEs with the same modification of 4 μL PtNPGNs/Nafion composite, a reproducibility within a mean value of ±5% was generally achieved for

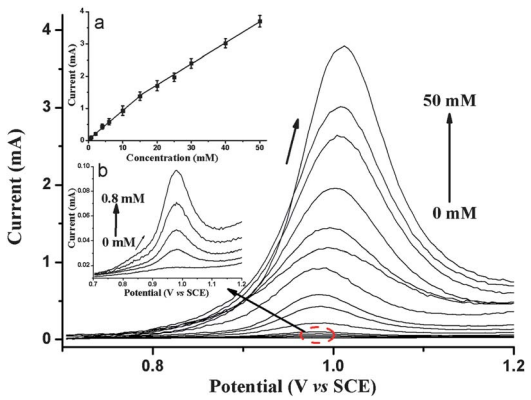

Fig. 4 DPVs at the PtNPGNs/Nafion-GCE in 0.1 M $HClO_4$ containing different concentrations of OA. The inset shows the calibration curve for OA detection (a) and the enlarged DPVs of OA from 0 to 0.8 mM (b). DPV conditions: amplitude, 50 mV; pulse width, 20 ms; pulse period, 200 ms.

the DPV determination of 10 mM OA. The long-term storage stability of the present non-enzymatic OA sensor was studied over a week by monitoring its DPV response to 10 mM OA in 0.1 M $HClO_4$ with an intermittent usage (at 1 day intervals), and storage in air at room temperature when not in use. It was found that the response of the OA sensor gradually decreased to approximately 80% of its initial value within a week. By taking advantage of the well-dispersed, high-yield, "clean" surface of PtNPs, and the large surface area, high conductivity of the GNs, the PtNPGNs/Nafion-GCE revealed an excellent performance for OA determination. The advantages of the proposed sensor could also be supported by comparison with other OA sensors, as shown in Table S2.†

To further verify the extensive application and reliability of the OA sensor, it was applied in the determination of OA in spinach samples. As shown in Table S3,† varying amounts of OA was added to the spinach samples, the recovery ranges from 96.0% to 105.0%, and the relative standard deviation was between 2.04% and 5.31%. The results were satisfactory and indicated that the proposed non-enzymatic OA sensor can be used for OA determination in some samples.

Conclusions

In summary, this study proposes a novel and highly-effective non-enzymatic OA sensor based on a PtNPGNs/Nafion-modified electrode. By comparing with other PtNPs, the superior electrocatalytic activity of the advanced material can be attributed to two factors: (i) the "clean" surface of the PtNPs, which may offer more active sites in the electro-oxidation; (ii) GNs with high surface areas and that can improve the inductivity of the electrochemical sensor. Owing to these properties, the PtNPGNs/Nafion-modified electrode exhibits a distinctly good performance towards OA oxidation with a lower onset potential, higher oxidation current and more stable response compared to the majority of the other electrodes. It is the first time that PtNPGNs have been constructed and used in non-enzymatic OA sensing. This approach provides a new facile route to construct effective OA sensors, and may provide a promising way to detect other biologically important compounds. Further experiments, such as the practical applications of this novel sensor and the construction of non-enzymatic labels for ultrasensitive bioanalysis are underway.

Acknowledgements

XM Chen thanks the Japan Society for the Promotion of Science (JSPS) for the fellowship. This research work was financially supported by the National Natural Science Foundation of China (NSFC, no. 21175112) and the Science and Technology Planning Project of Fujian Province, China (2012Y0052), which are gratefully acknowledged.

Notes and references

1 A. I. Tribidasari, N. R. Tata, F. Akira and E. Yasuaki, *Anal. Chem.*, 2006, **78**, 3467.
2 C. S. Pundir, N. Chauhan, Rajneesh, M. Verma and Ravi, *Sens. Actuators, B*, 2011, **155**, 796.
3 F. Hong, N. O. Nilvebrant and L. J. Jönsson, *Biosens. Bioelectron.*, 2003, **18**, 1173.
4 T. E. Benavidez, R. H. Capra, C. I. Alvarez and A. M. Baruzzi, *Electroanalysis*, 2009, **21**, 837.
5 L. M. Santos and R. P. Baldwin, *Anal. Chem.*, 1986, **58**, 848.
6 L. G. Shaidarova, A. V. Gedmina, I. A. Cheinokova and G. K. Budnikov, *J. Anal. Chem.*, 2003, **58**, 886.
7 H. Ahmar, A. R. Fakhari, M. R. Nabid, S. Jamal, T. Rezaei and Y. Bide, *Sens. Actuators, B*, 2012, **171–172**, 611.
8 T. C. Canevari, J. Arguello, M. S. P. Francisco and Y. Gushikem, *J. Electroanal. Chem.*, 2007, **609**, 61.
9 Y. Q. Zheng, C. Z. Yang, W. H. Pu and J. D. Zhang, *Food Chem.*, 2009, **114**, 1523.
10 A. Rahim, S. B. A. Barros, L. T. Arenas and Y. Gushikem, *Electrochim. Acta*, 2011, **56**, 1256.
11 M. J. Chollier-Brym, F. Epron, E. Lamy-Pitara and J. Barbier, *J. Electroanal. Chem.*, 1999, **474**, 147.
12 S. N. Pron'kin, O. A. Petrii, G. A. Tsirlina and D. J. Schiffrin, *J. Electroanal. Chem.*, 2000, **480**, 112.
13 L. C. Rockombeny, J. P. Feraud, B. Queffelec, D. Ode and T. Tzedakis, *Electrochim. Acta*, 2012, **66**, 230.
14 H. J. Wang, M. Imura, Y. Nemoto, S. E. Park and Y. Yamauchi, *Chem.–Asian J.*, 2012, **7**, 802.
15 J. Y. Shin, Y. S. Kim, Y. Lee, J. H. Shim, C. Lee and S. G. Lee, *Chem.–Asian J.*, 2011, **6**, 2016.
16 S. J. Guo, D. Wen, Y. M. Zhai, S. J. Dong and E. K. Wang, *ACS Nano*, 2010, **4**, 3959.
17 E. Yoo, T. Okata, T. Akita, M. Kohyama, J. Nakamura and I. Honma, *Nano Lett.*, 2009, **9**, 2255.
18 X. M. Chen, G. H. Wu, Y. Q. Jiang, Y. R. Wang and X. Chen, *Analyst*, 2011, **136**, 4631.
19 V. Georgakilas, M. Otyepka, A. B. Bourlinos, V. Chandra, N. Kim, K. C. Kemp, P. Hobza, R. Zboril and K. S. Kim, *Chem. Rev.*, 2012, **112**, 6156.
20 A. Mondal, A. Sinha, A. Saha and N. R. Jana, *Chem.–Asian J.*, 2012, **7**, 2931.
21 S. L. Hu, Y. G. Dong, J. L. Yang, J. Liu, F. Tian and S. R. Cao, *Chem.–Asian J.*, 2012, **7**, 2711.
22 S. J. Guo and S. H. Sun, *J. Am. Chem. Soc.*, 2012, **134**, 2492.
23 X. M. Chen, G. H. Wu, J. M. Chen, X. Chen, Z. X. Xie and X. R. Wang, *J. Am. Chem. Soc.*, 2011, **133**, 3693.
24 X. M. Chen, B. Y. Su, G. H. Wu, C. J. Yang, Z. X. Zhuang and X. Chen, *J. Mater. Chem.*, 2012, **22**, 11284.
25 S. William, J. Hummers and R. Offeman, *J. Am. Chem. Soc.*, 1958, **80**, 1339.
26 L. J. Cote, F. Kim and J. Huang, *J. Am. Chem. Soc.*, 2009, **131**, 1043.
27 Z. Lin, Y. Yao, Z. Li, Y. Liu and C. P. Wong, *J. Phys. Chem. C*, 2010, **114**, 14819.
28 I. G. Casella, *Electrochim. Acta*, 1999, **44**, 3353.
29 C. A. Martınez-Huitle, S. Ferro and A. D. Battisti, *Electrochim. Acta*, 2004, **49**, 4027.
30 Y. Liu, J. S. Huang, D. W. Wang, H. Q. Hou and T. Y. You, *Anal. Methods*, 2010, **2**, 855.